UCRL-11374 Rev

University of California

Ernest O. Lawrence Radiation Laboratory

CORRELATIONS BETWEEN PHOTOINDUCED EPR AND PHOTOCONDUCTIVITY IN TONE-THF SOLUTION CHARGE-TRANSFER COMPLEX

Berkeley, California

Submitted to Journal of Chemical Physics

UCRL-11374 Rev

UNIVERSITY OF CALIFORNIA

Lawrence Radiation Laboratory
Berkeley, California

AEC Contract No. W-7405-eng-48

CORRELATIONS BETWEEN PHOTOINDUCED EPR AND PHOTOCONDUCTIVITY IN TONE-THF SOLUTION CHARGE-TRANSFER COMPLEX

David F. Ilten and Melvin Calvin

December 8, 1964

UCRL-11374 Rev

CORRELATIONS BETWEEN PHOTOINDUCED EPR AND PHOTOCONDUCTIVITY IN TCNE-THF SOLUTION CHARGE-TRANSFER COMPLEX

David F. Ilten* and Melvin Calvin

Lawrence Radiation Laboratory, University of California,

Berkeley, California

December 8, 1964

Abstract

Reversible photoinduced electron paramagnetic resonance (EPR) signals and photoconductivity were observed when a solution of tetracyanoethylene (TCNE) in tetrahydrofuran (THF) was irradiated in the charge-transfer band of the complex formed between these two compounds. The eleven-line hyperfine structure of the EPR spectrum which was obtained demonstrated the presence of TCNE negative ion radical. The concentration of this radical was found to be directly proportional to the square root of the light intensity. Second order decay kinetics were followed when the light was shut off. Both the EPR signal and the photoconductivity rose initially as the square of the time. The latter portions of the growth curves could be fit to the latter portions of a hyperbolic tangential growth curve. From these data a reaction mechanism was proposed. The rate law

$$dn/dt + kn^2 - \alpha L(1-e^{-\beta t}) = 0,$$

where n = the concentration of radicals, t = the time, k, α, and β are rate constants, and L = the light intensity, described both the photoinduced EPR and the photoconductivity within the limits of experimental accuracy.

---

*National Institutes of Health Predoctoral Fellow, 1960-1964.

INTRODUCTION

In 1958 Sogo, Tollin, and Calvin[1] postulated that the oxidative and the reductive processes of photosynthesis could take place at separated sites in plants. These processes are preceded by a photo-induced transfer of an electron from a donor site to an acceptor site. During the past few years much effort has been expended in determining the conditions required for such an electron transfer between donors and acceptors in solids.[2] More recently Lagercrantz and Yhland[3,4,5] have used EPR to demonstrate the photoinduced transfer of an electron between donors and acceptors in solutions. The present work is an attempt to correlate photoinduced EPR with photoconductivity for a solution composed of organic donor and acceptor molecules.

Tetracyanoethylene (TCNE), a colorless cyanocarbon, was first prepared by Cairns, et al.[6] in 1958. At that time Merrifield and Phillips[7] reported that TCNE readily dissolves in many organic solvents to produce intensely colored solutions. The colors were attributed, after Mulliken[8,9,10] to the formation of intermolecular charge-transfer complexes between the organic solvent donor molecules and the TCNE acceptor molecules. As is indicated by the spectra in Fig. 1, TCNE forms a charge-transfer complex with tetrahydrofuran (THF). Fig. 1a shows the spectrum of TCNE in ethylene dichloride, with maxima at 2650 Å and 2750 Å. The spectrum of TCNE in THF is shown in Fig. 1b. Here the two TCNE bands have been shifted to 2630 Å and 2710 Å, respectively, and a third band has appeared at 3000 Å. This latter band is characteristic of the charge-transfer complex. Vars, Tripp, and Pickett[11] studied the TCNE-THF complex in chloroform solution and

found the maximum to occur at 3100 Å. This shift is not unexpected, as Mulliken's theory predicts an effect of the dielectric constant of the solution on the position of the absorption maximum of the complex. TCNE negative ion radicals, as detected by EPR, can be produced by irradiating a solution of TCNE-THF with a mercury lamp. This was first reported by Ward.[12] In this present work, studies of the dependence of the EPR signal level on the intensity and the wavelength of the incident light were carried out. The reversible photoinduced EPR suggested that photoconductivity might be seen as well. This was, in fact, observed.

EXPERIMENTAL

Eastman Kodak tetrahydrofuran was initially dried with potassium hydroxide pellets and then treated with lithium aluminum hydride. This sample was refluxed for two hours and then distilled. The first 100 ml portion of the distillate was discarded. The portion collected boiled at 65.5° C. Eastman Kodak White Label tetracyanoethylene was used without further treatment. All measurements were made on freshly-prepared solutions.

APPARATUS AND PROCEDURE

The EPR data were obtained using a microwave spectrometer consisting of a 9 gigacycle/second klystron, a reflection cavity, and a crystal detection unit. The spectrometer magnet, which had been constructed in this laboratory, had pole pieces 6 inches in diameter and was powered with a Varian V2200 magnet power supply. A Varian 4560 100 kilocycle/second phase sensitive field modulation unit was used for crystal detection. A 60 kilocycle/second automatic frequency control unit that had been constructed in this laboratory was used. The measurements were made in a Varian V4531 rectangular cavity ($TE_{c/2}$ mode)

with slots for irradiation. The spectrometer was calibrated by comparing the observed signal with a standard of 5×10^{14} spins of Cr^{+++} in an MgO host. The g-value for the standard was approximately 2.0023.

Photoconductivity Apparatus

A block diagram of the photoconductivity apparatus is shown in Fig. 2. The direct current resistance was measured by applying a fixed voltage to the sample and simultaneously measuring the current flow with a picoammeter (Keithley Model 410). The voltage supply consisted of a 90-volt direct current source in series with a variable resistance, so that the applied potential could be varied from 0 to 90 volts. In almost all cases the applied potential was less than one volt. A General Radio Type 1809-A vacuum tube volt meter was used for potential measurements. The 0 to 65% rise-time of the Keithley 410 picoammeter was 0.001 second. However, the Sanborn Recorder used to record the ammeter output had a 0 to 100% rise-time of 0.01 second. The effects observed were long in comparison.

Light Sources

The light source for both the photoconductivity and the photoinduced EPR was a Westinghouse H33-1-CD 400 watt mercury vapor lamp focused onto the slots of the EPR cavity or onto the conductivity cell by two glass lenses. The glass case of the lamp cut off all wavelengths shorter than 3100 Å. The total rated output from 3100 Å to 3500 Å was 0.54 watts.[13] This corresponded to 1.6×10^{16} quanta per second, assuming 3300 Å quanta. From 3500 Å to 4500 Å the output was 30.2 watts, or, assuming 4000 Å quanta, 6×10^{19} quanta/second. Cut-off filters were used to determine which wavelengths were producing the photoeffects. The

intensity of the irradiation was varied by inserting a series of neutral density filters between the light source and the sample. These were of nominal transmission values of 5%, 25%, and 50%. The filters were calibrated using a Cary 14R recording spectrophotometer and were found to have transmission values of 4.7%, 22%, and 47.5%. It was estimated that 1% of the rated intensity of the lamp reached the sample in the case of the photoconductivity experiments. Because of differences in the geometry, the light intensity for photoinduced EPR was approximately a factor of five smaller than that in the case of the photoconductivity. This intensity difference was measured with a photodiode.

RESULTS

The results of these investigations are presented in Figs. 3-13. The data in Figs. 3-6 indicate that the steady-state EPR signal is dependent upon the square root of the light intensity, that the decay of the signal is second order, and that the signal grows for several minutes as the square of the time. The final portion of the EPR curve (not shown) can be fit to the final portion of a hyperbolic tangential rise curve. The photoconductivity results are given in Figs. 7-13. Again, the steady-state signal is dependent upon the square root of the light intensity, the decay is second order, and the rise goes for several minutes as the square of the time, but finally grows as the hyperbolic tangent of the time.

DISCUSSION

On the basis of these data, the following reaction mechanism was proposed for the formation of the TCNE negative ion radical:

Because of the large excess of THF, it was assumed that essentially all of the TCNE molecules were complexed

$$D + A \rightleftharpoons C \qquad (1a)$$

The complex is excited to the excited singlet state by an incident photon, a process which is directly proportional to L, the light intensity absorbed.

$$C \xrightarrow{L} C^S \qquad (1b)$$

The complex in the excited singlet state relaxes to the ground state. This process proceeds according to a first order rate law, with a rate constant k_2.

$$C^S \xrightarrow{k_2} C \quad \text{(plus energy)} \qquad (1c)$$

The excited singlet state goes to the excited triplet state. The first order rate constant is k_3.

$$C^S \xrightarrow{k_3} C^T \qquad (1d)$$

The excited triplet state of the complex returns to the ground state. The rate constant is k_4.

$$C^T \xrightarrow{k_4} C \qquad (1e)$$

The triplet state of the complex goes to the ionized components of the complex, D^+ and A^-. The rate constant is k_5.

$$C^T \xrightarrow{k_5} D^{\oplus} + A^{\ominus} \qquad (1f)$$

The ions recombine to form the complex. The second order rate constant is k_6.

$$D^+ + A^- \xrightarrow{k_6} C \qquad (1g)$$

An expression for the rate of change of the concentration of the TCNE negative ion radicals can be obtained from equations (1f) and (1g)

$$dn/dt = k_5 c^T - k_6 n^2 \qquad (2)$$

where

c^T = the concentration of molecules in the triplet excited state,

n = the concentration of TCNE negative ion radicals.

By assuming the concentration of the singlet species, c^S, to be at a steady state,

$$dc^S/dt = L - (k_2 + k_3)\, c^S = 0, \text{ or}$$

$$c^S = L/(k_2 + k_3) .$$

By similar arguments, using equations (1d), (1e), and (1f), expressions are obtained for the rate of change of the concentration of the species in the triplet state,

$$dc^T/dt = k_3 c^S - (k_4 + k_5) c^T, \qquad (3)$$

$$dc^T/dt = k_3 L/(k_2 + k_3) - (k_4 + k_5) c^T \qquad (4)$$

When equation (4) is integrated, an expression is obtained for c^T, the concentration of the species in the triplet state,

$$c^T = \frac{k_3 L}{(k_2 + k_3)(k_4 + k_5)} \left(1 - e^{-(k_4 + k_5)\, t}\right) . \qquad (5)$$

An expression for n, the concentration of the negative ion radical species (in this case, $TCNE^-$), can be obtained from (1f) and (1g), as in equation (2),

$$dn/dt = k_5 c^T - k_6 n^2 . \qquad (6)$$

In attempting to obtain a solution to equation (6), it is helpful to consider three cases.

Case (1). The light intensity goes to zero. The c^T goes to zero, and (6) becomes

$$dn/dt = -k_6 n^2, \qquad (7)$$

which is the equation for second order decay.

Case (2). The steady state. At the steady state, $t = t_{ss}$ and

$$c^T = \frac{k_3 L}{(k_2 + k_3)(k_4 + k_5)} \left(1 - e^{-(k_4 + k_5)\, t_{ss}}\right) \qquad (8)$$

Since t_{ss} is large, equation (8) becomes

$$c^T = \frac{k_3 L}{(k_2 + k_3)(k_4 + k_5)} \qquad (9)$$

However, it can be seen from equation (6) that at the steady state

$$n^2 = (k_5/k_6)\, c^T \qquad \text{or}$$

$$n_{ss} = L^{1/2} \left(\frac{k_3\, k_5}{(k_2 + k_3)(k_4 + k_5)k_6}\right)^{1/2}$$

Therefore, the steady-state concentration of spins is dependent upon the square root of the light intensity.

Case (3). The rise time.

The rate of increase of the concentration of n is given by

$$dn/dt = \frac{L\, k_3\, k_5}{(k_2 + k_3)(k_4 + k_5)} \left(1 - e^{-(k_4 + k_5)t}\right) - k_6\, n^2 \qquad (10)$$

By letting

$$\alpha = \frac{k_3\, k_5}{(k_2 + k_3)(k_4 + k_5)}, \qquad \beta = (k_4 + k_5),$$

expression (10) becomes

$$dn/dt = \alpha\, L(1 - e^{-\beta t}) - k_6\, n^2$$

or

$$dn/dt + k_6\, n^2 - \alpha\, L(1 - e^{-\beta t}) = 0 \qquad (11)$$

Equation (11) is a first-order non-linear differential equation which cannot in general be solved in closed form. It is an example of Riccati's Equation. Certain Riccati Equations can be transformed into second-order linear equations and then solved.[14] Since equation (11) is not susceptible to this approach, certain simplifying assumptions are made.

(1) When the light is first turned on, n = 0, so that equation (11) becomes

$$dn/dt - \alpha L(1 - e^{-\beta t}) = 0 \quad .$$

This can be integrated to

$$n = \alpha\beta\, t + e^{-\beta t} - 1$$

For small t, $e^{-\beta t} = 1 - \beta t + \beta^2 t^2$

or

$$n = \beta^2 t^2 + t(\alpha L - 1) \quad ,$$

indicating a parabolic rise of the concentration of unpaired electrons with time.

At large t,

$$dn/dt = \alpha L - k_6 n^2$$

$$n = n_{ss} \tanh \left[\left(\frac{k_6}{\alpha} \right)^{1/2} L^{1/2} t \right] \quad ,$$

which predicts a rise of the EPR photosignal as the hyperbolic tangent of time.

Assumptions involved in Photoconductivity Calculations.

The conductivity may be expressed as $\sigma = pe\mu_p + ne\mu_n$,

where p and n are the concentration of the positive and negative charge carriers respectively, e is the charge of the electron, and μ_n and μ_p are the mobilities of the positive and the negative carriers. The following assumptions are then made:

(1) Each carrier bears unit charge.

(2) The mobility of the charge carriers is independent of the concentration of the carriers and is essentially the same for positive and negative carriers.

(3) The conductivity is ionic. For each TCNE negative ion radical formed a THF positive ion radical is formed as well.

Because $p = n$ and $\mu_n \sim \mu_p$, $\sigma = 2ne\mu$.

The mobility, μ, is defined as $v/\mathcal{E}$, so $v = \sigma\mathcal{E}/2ne$.

Calculation of Ionic Velocities from Experimental Data.

From EPR data there are approximately 5.75×10^{15} carriers/cm^3. The conductivity, σ, is 2.33×10^{-6} ohm^{-1} cm^{-1} when the applied voltage is 0.18 volts/cm.

$v = \sigma\mathcal{E}/2ne = 5 \times 10^{-5}$ cm/sec .

Calculation of Ionic Velocities from Stokes' Law.

By equating the electrostatic attractive force exerted by a field on a charged sphere to the retarding force due to the viscosity of the medium, the relation

$eE = 6\pi\eta av$ is obtained

where

η = the intrinsic viscosity of the medium (THF) = 0.0107 Stokes at 25° C,[15]

a = the ionic radius, estimated at 3.20 Å

$e = 6 \times 10^{-10}$ esu, the charge on the electron,

E = the electric field in statvolts/cm = $300\mathcal{E}$.

From this expression a value for the ionic velocity, $v = 6.5 \times 10^{-5}$ cm/sec is calculated.

It has been assumed in the above arguments that the THF positive ion radical was formed. However, it was not detected by EPR. The absence of a THF^+ spin signal may be explained by an argument presented

by Eastman.[16] It should be noted that there is a large excess of THF neutral molecules over THF positive ion radicals, and that holes are free to migrate from THF^+ to THF neutral species. A hole migration throughout the solution would be expected to lead to a broadening of the EPR signal so that it would become undetectable. Other similar cases of the observation of only a single radical have been reported.[17] The temperature dependence of the conductivity could give corroborating evidence for a hole migration process. Were the conductivity purely ionic, its change with change in temperature should be approximately as the change of the viscosity of the medium with changing temperature. If a hole migration process with a relatively high energy barrier is possible, a change in conductivity with a change in temperature greater than the change in viscosity is to be expected.

SUMMARY

Evidence for the reversible photoinduced transfer of an electron from a THF donor molecule to a TCNE acceptor has been obtained from photo-EPR and photoconductivity measurements. One of the radicals formed was identified from the hyperfine splitting of the EPR signal to be TCNE negative ion radical. Calculations of the ionic velocities from EPR and conductivity data gave a reasonable agreement with values obtained from calculations based on Stokes' Law. The THF positive ion radical was not detected by EPR. A possible explanation for this is that the signal was broadened by exchange so that it became undetectable.

ACKNOWLEDGMENTS

We wish to thank the members of the Bio-Organic Chemistry Group for many helpful discussions.

This work was supported, in part, by the U. S. Atomic Energy Commission.

One of us (D.F.I.) wishes to thank the National Institutes of Health for a predoctoral fellowship.

REFERENCES

1. G. Tollin, P. B. Sogo, and M. Calvin, Ann. N. Y. Acad. Sci. 74, 310 (1958).

2. J. Eastman, G. Androes, and M. Calvin, J. Chem. Phys. 36, 1197 (1962).

3. C. Lagercrantz and M. Yhland, Acta Chem. Scand. 16, 1043 (1962).

4. C. Lagercrantz and M. Yhland, ibid. 16, 1799 (1962).

5. C. Lagercrantz and M. Yhland, ibid. 16, 1807 (1962).

6. T. L. Cairns, et al., J. Am. Chem. Soc. 80, 2775 (1958).

7. R. E. Merrifield and W. D. Phillips, ibid. 80, 2778 (1958).

8. R. S. Mulliken, J. Chem. Phys. 19, 514 (1961).

9. R. S. Mulliken, J. Phys. Chem. 56, 801 (1952).

10. R. S. Mulliken, J. Am. Chem. Soc. 74, 811 (1952).

11. R. Vars, L. A. Tripp, and L. W. Pickett, J. Phys. Chem. 66, 1754 (1963).

12. R. Ward, J. Chem. Phys. 39, 852 (1963).

13. R. B. Withrow and A. P. Withrow, in Radiation Biology (A. Hollaender, Ed.), McGraw-Hill, New York, London, Toronto, 1956, Vol. III, p. 173.

14. E. Kamke, Differential Gleichungen, 2nd Ed., Akademische Verlagsgesellschaft, Becker and Erler, Rome-Leipzig, 1943, Vol. I, p. 21.

15. F. Thole, J. Chem. Soc. (London), 105, 2004 (1914).

16. J. W. Eastman, G. M. Androes, and M. Calvin, Nature 193, 1067 (1962).

17. W. D. Phillips, J. C. Rowell, and S. I. Weissman, J. Chem. Phys. 33, 626 (1960).

Figure 1. Optical Absorption Spectra demonstrating the formation of a charge-transfer complex between tetracyanoethylene and tetrahydrofuran. a. 2×10^{-5} M TCNE in CCl_4. b. 2×10^{-5} M TCNE in THF. c. 0.01 M TCNE in THF.

Figure 2. Photoconductivity apparatus. a. Block diagram of the measuring device. b. Conductivity cell (metal shielding is not shown).

Figure 3. A linear plot of the steady-state value of the EPR photosignal for 0.01 M TCNE in THF versus the relative light intensity.

Figure 4. The steady-state value of EPR photosignal for a solution of 0.01 M TCNE in THF as a function of the light intensity. The log of the steady-state signal is plotted against the log of the light intensity.

Figure 5. Decay of the EPR photosignal for 0.01 M TCNE in THF. a. Linear plot of EPR photosignal versus time. b. The reciprocal of the EPR photosignal versus time. The linear relation for b indicated that second order decay kinetics are followed.

Figure 6. Growth of the EPR photosignal for 0.01 M TCNE in THF. The signal level is plotted against the square of the time.

Figure 7. Steady-state photocurrent versus light intensity for 0.01 M TCNE in THF. a. Steady-state photocurrent versus relative light intensity. b. Steady-state photocurrent versus the square root of the relative light intensity. The applied potential was 0.09 volts.

Figure 8. Steady-state photocurrent for 0.01 M TCNE in THF versus the log of the relative light intensity. The applied potential was 0.09 volts.

Figure 9. Decay of the photocurrent for 0.01 M TCNE in THF. The reciprocal of the photocurrent is plotted against the time of decay. 0.09 volts is the applied potential.

Figure 10. Decay of the photocurrent for 0.01 M TCNE in THF. The log of the photocurrent is plotted against the time of decay. First order decay is not followed.

Figure 11. Growth curve for the photoconductivity of 0.01 M TCNE in THF. (Signal level)/(Steady-state signal level) is plotted against time. The black dots indicate the hyperbolic tangent of 0.12t. The applied potential was 0.09 volts.

Figure 12. The growth of the photocurrent for 0.01 M TCNE in THF. The inverse hyperbolic tangent of (photocurrent/steady-state photocurrent) is plotted against time. The applied potential was 0.09 volts.

Figure 13. Maximum photocurrent for 0.01 M TCNE in THF as a function of the applied voltage.

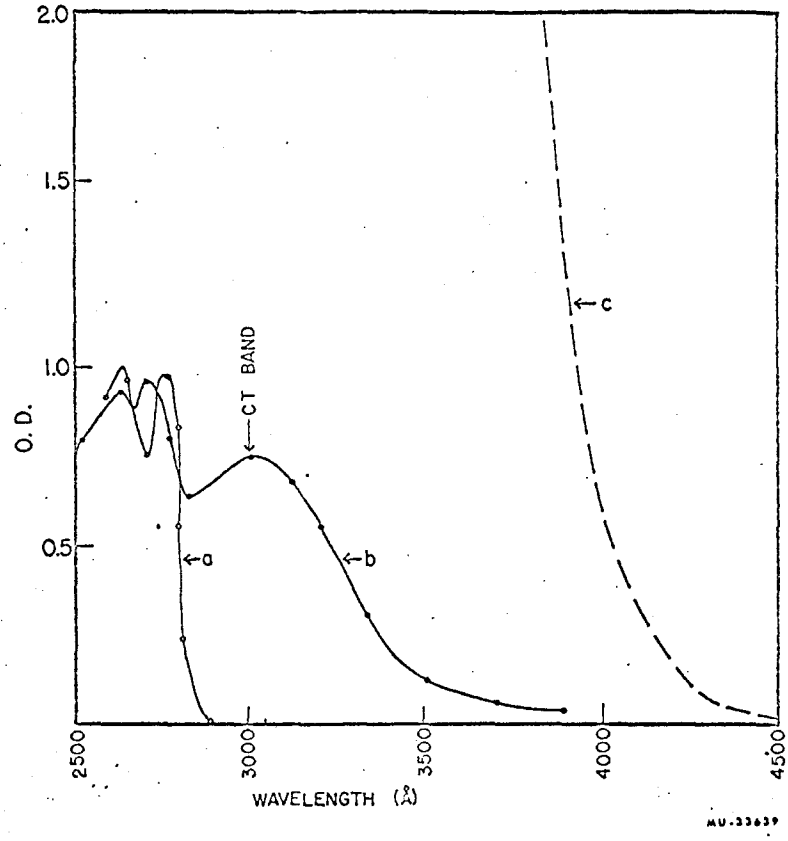
2.0
1.5
1.0
0.5
O. D.
CT BAND
←a
←b
←c
2500
3000
3500
4000
4500
WAVELENGTH (Å)
MU-33639

Fig. 1

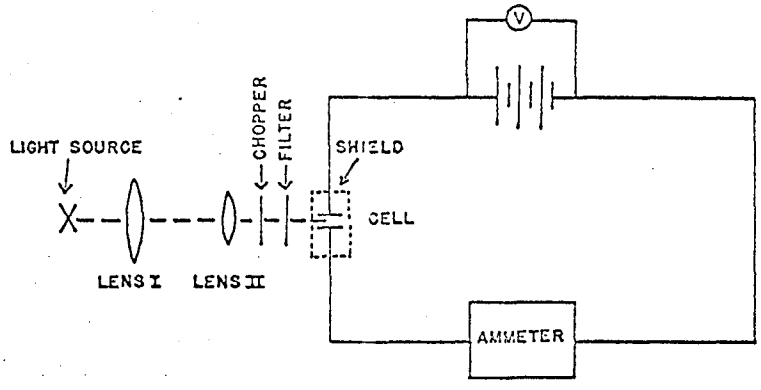

PHOTOCONDUCTIVITY APPARATUS

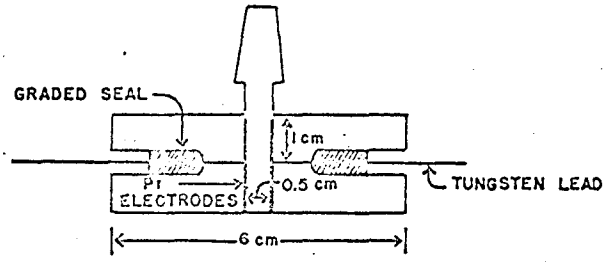

QUARTZ CONDUCTIVITY CELL

MU-33653

Fig. 2

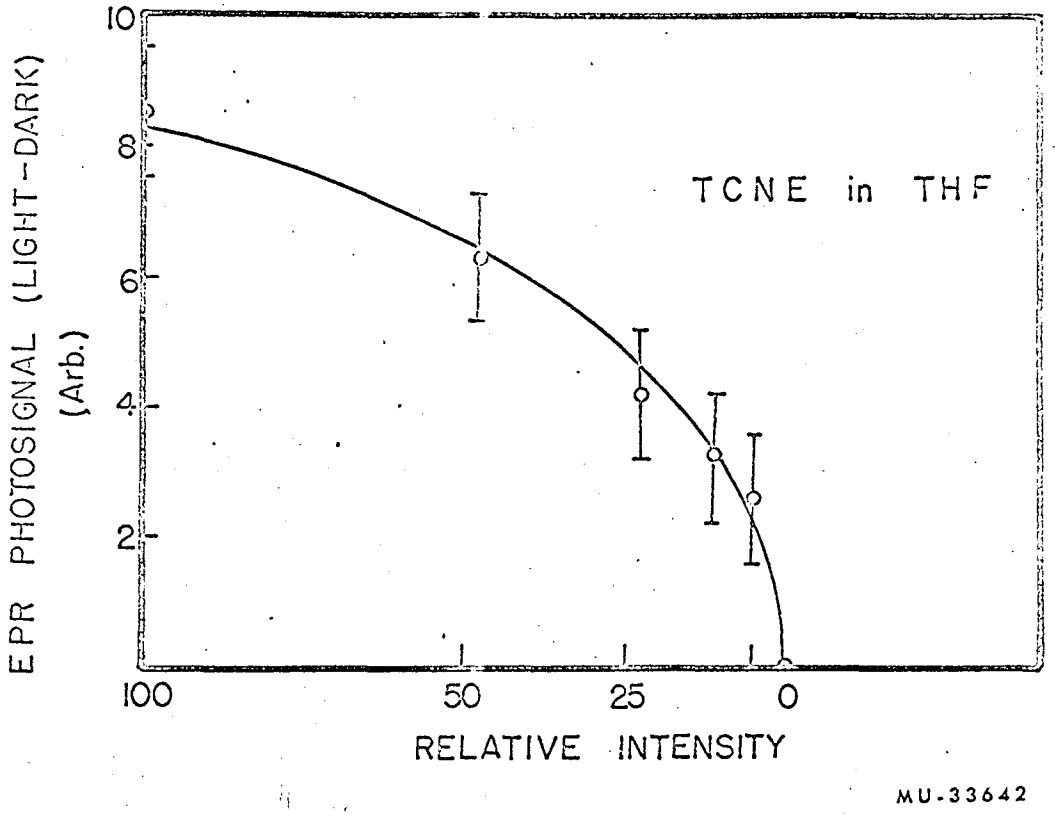
EPR PHOTOSIGNAL (LIGHT-DARK)
(Arb.)
10
8
6
4
2
TCNE in THF
100
50
25
0
RELATIVE INTENSITY
MU-33642

Fig. 3

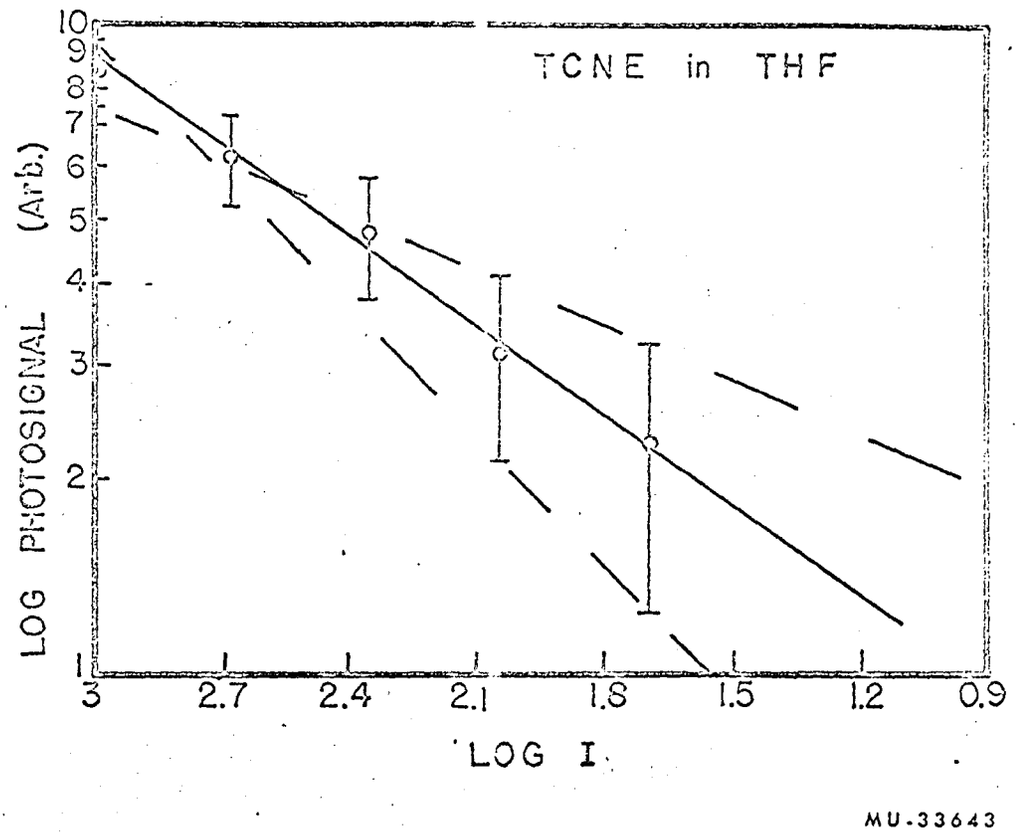
TCNE in THF
LOG PHOTOSIGNAL (Arb.)
10
9
8
7
6
5
4
3
2
1
3
2.7
2.4
2.1
1.8
1.5
1.2
0.9
LOG I
MU-33643

Fig. 4

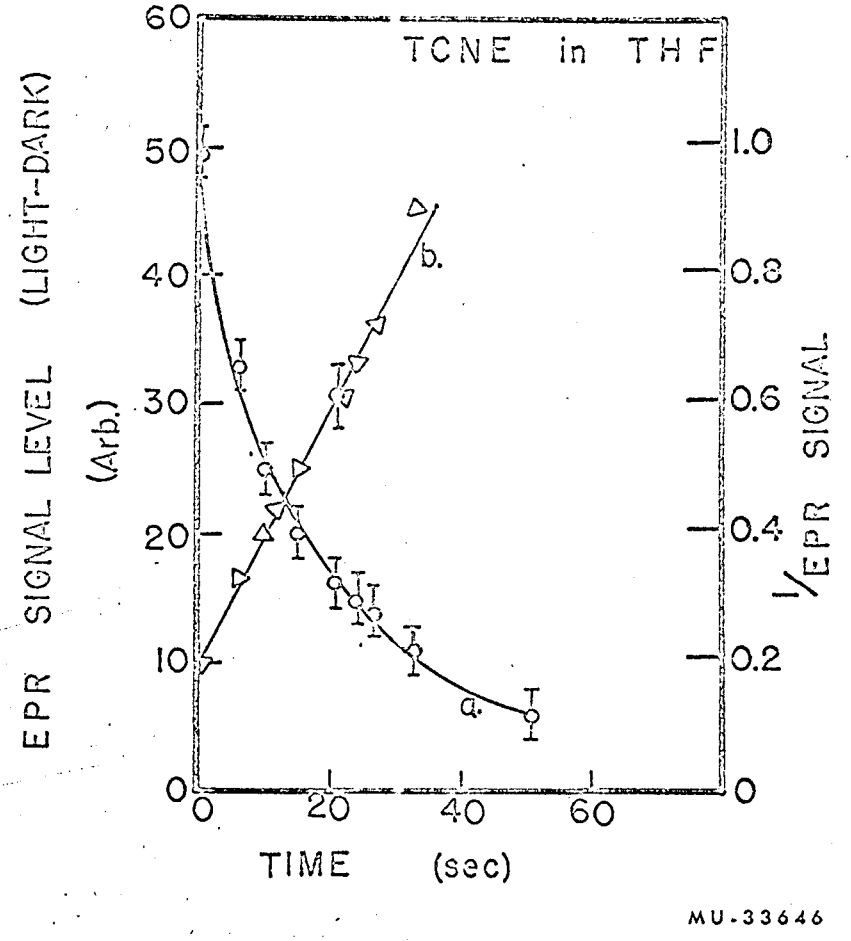
TCNE in THF
EPR SIGNAL LEVEL (LIGHT-DARK)
(Arb.)
1/EPR SIGNAL
TIME (sec)
a.
b.
0
10
20
30
40
50
60
0.2
0.4
0.6
0.8
1.0
0
20
40
60
MU-33646

Fig. 5

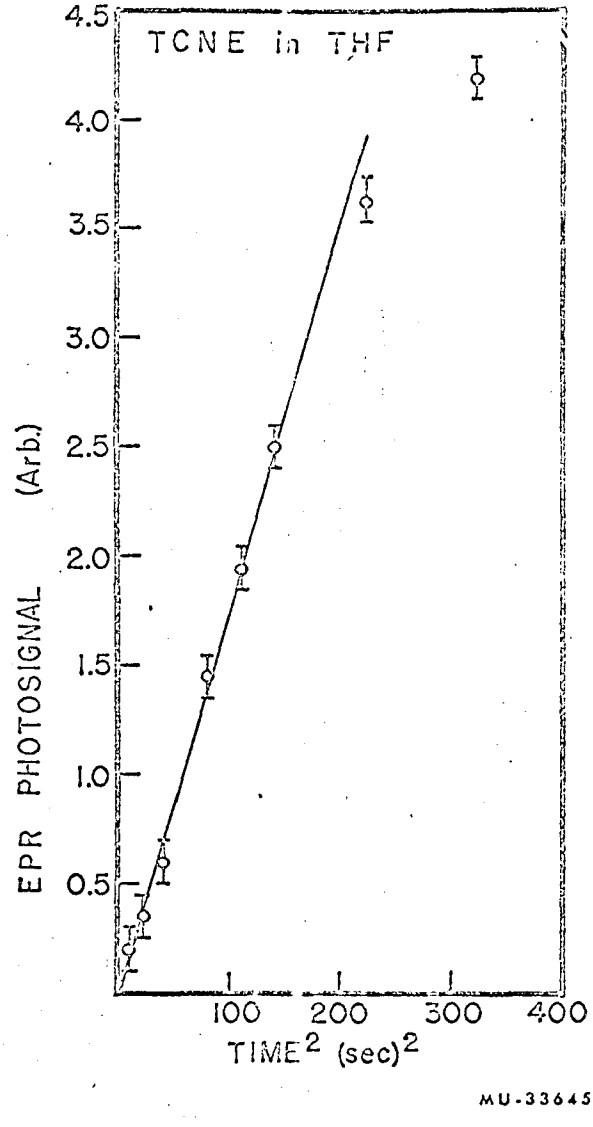
TCNE in THF
EPR PHOTOSIGNAL (Arb.)
4.5
4.0
3.5
3.0
2.5
2.0
1.5
1.0
0.5
100
200
300
400
TIME^2 (sec)^2
MU-33645

Fig. 6

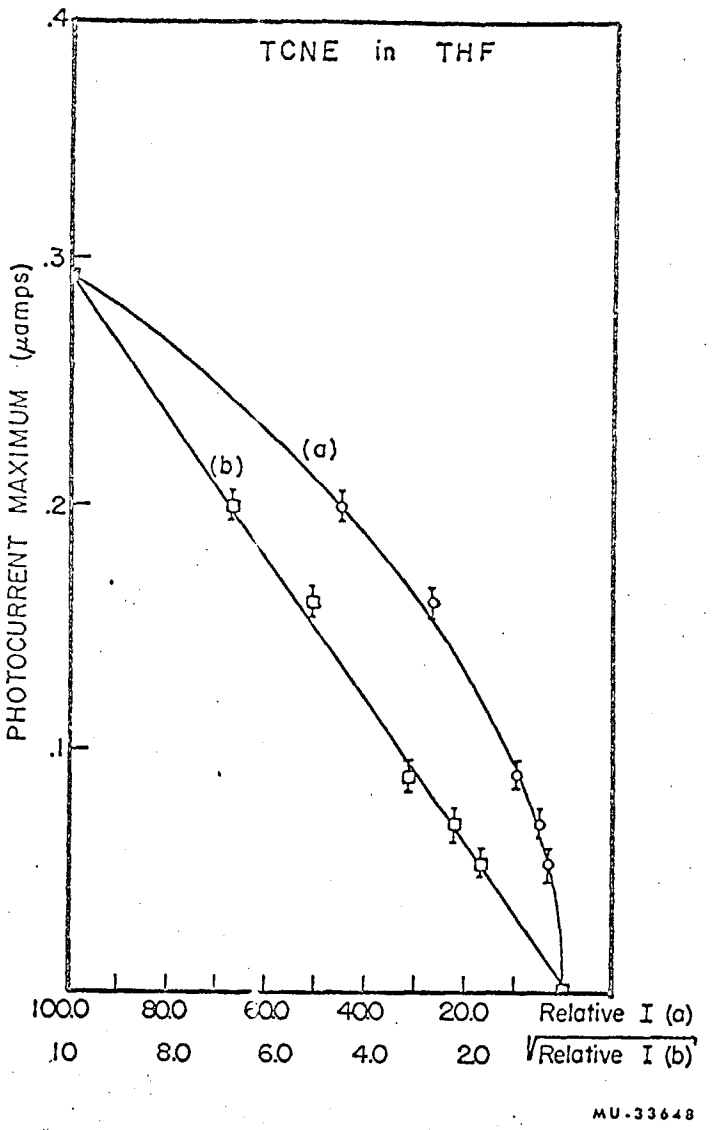
TCNE in THF
PHOTOCURRENT MAXIMUM (μamps)
.4
.3
.2
.1
(a)
(b)
100.0
80.0
60.0
40.0
20.0
Relative I (a)
10
8.0
6.0
4.0
2.0
√Relative I (b)
MU-33648

Fig. 7

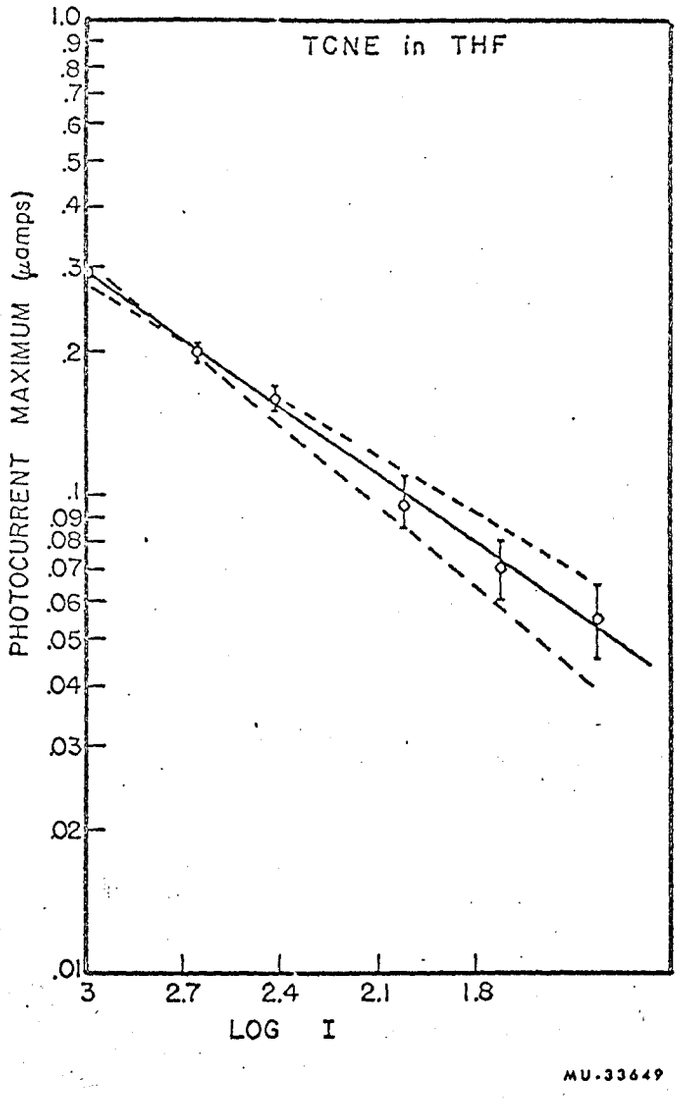
TCNE in THF
PHOTOCURRENT MAXIMUM (μamps)
1.0
.9
.8
.7
.6
.5
.4
.3
.2
.1
.09
.08
.07
.06
.05
.04
.03
.02
.01
3
2.7
2.4
2.1
1.8
LOG I
MU-33649

Fig. 8

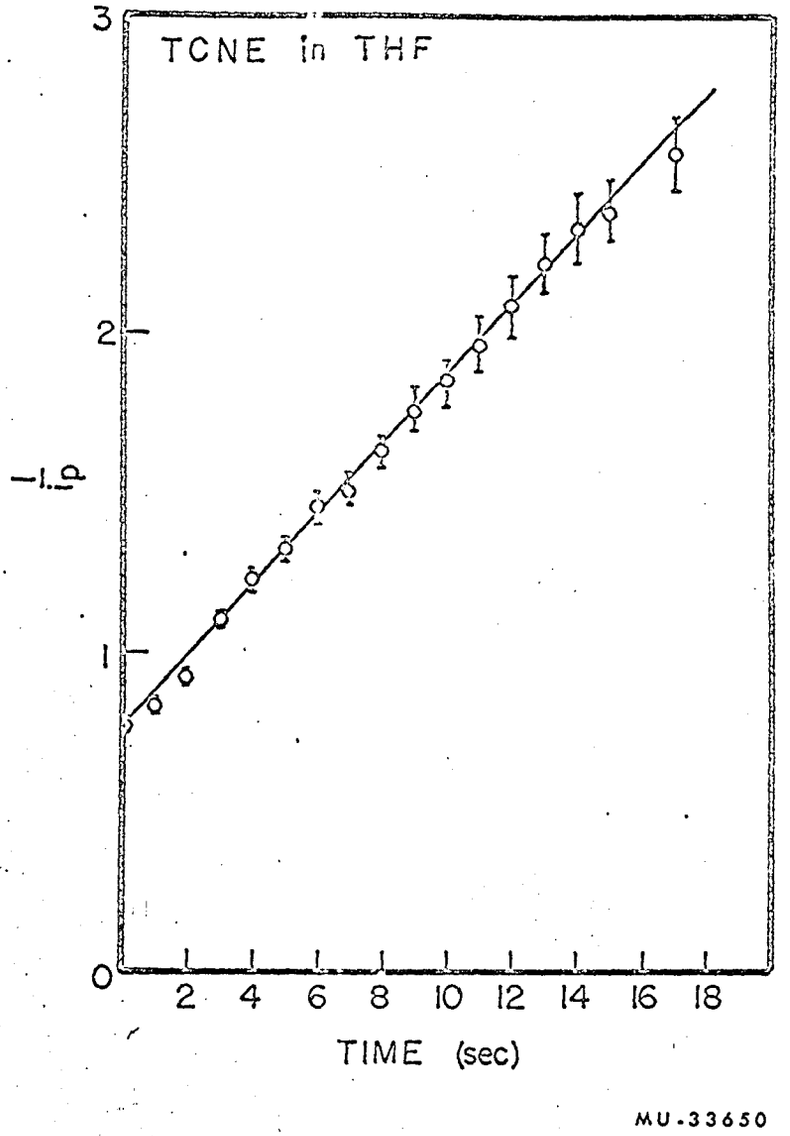

Fig. 9

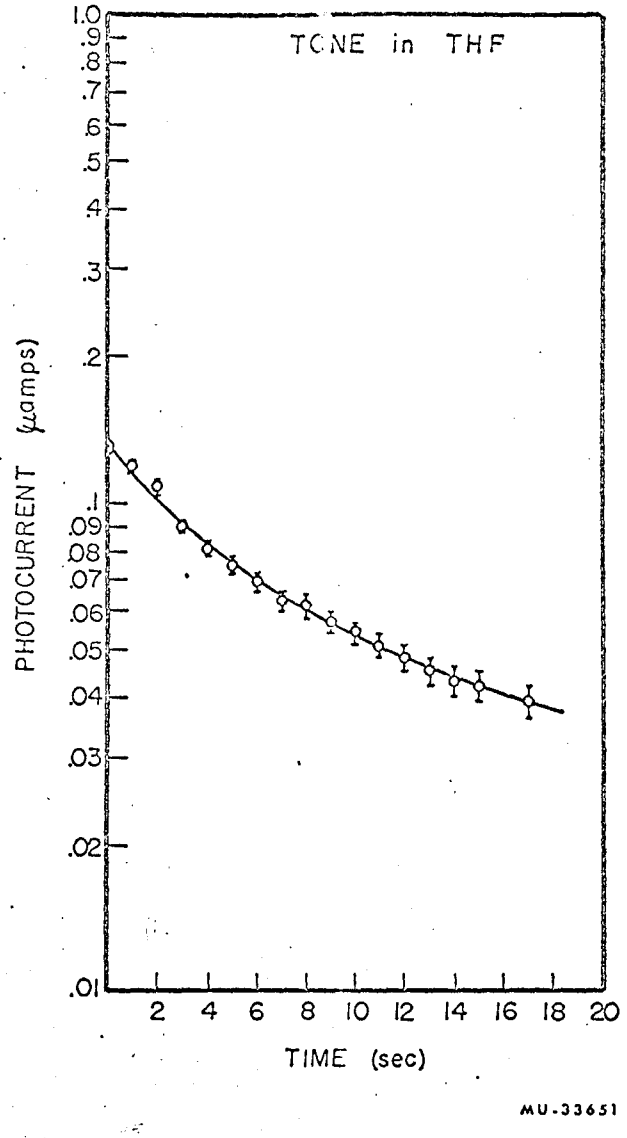
TCNE in THF
PHOTOCURRENT (μamps)
1.0
.9
.8
.7
.6
.5
.4
.3
.2
.1
.09
.08
.07
.06
.05
.04
.03
.02
.01
2
4
6
8
10
12
14
16
18
20
TIME (sec)
MU-33651

Fig. 10

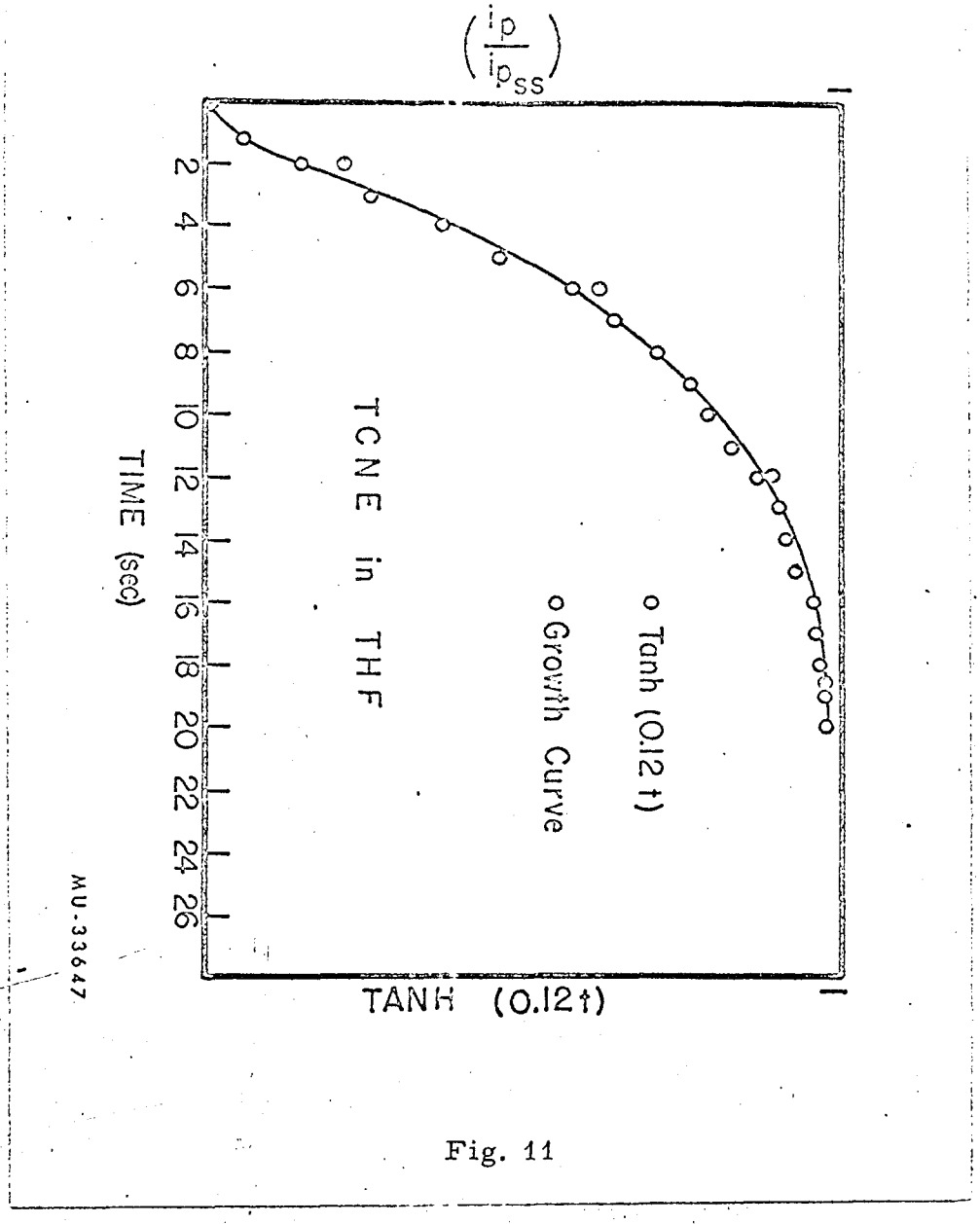
$\left(\frac{i_p}{i_{p_{ss}}}\right)$
1
2
4
6
8
10
12
14
16
18
20
22
24
26
TIME (sec)
TCNE in THF
o Tanh (0.12 t)
o Growth Curve
TANH (0.12t)
MU-33647

Fig. 11

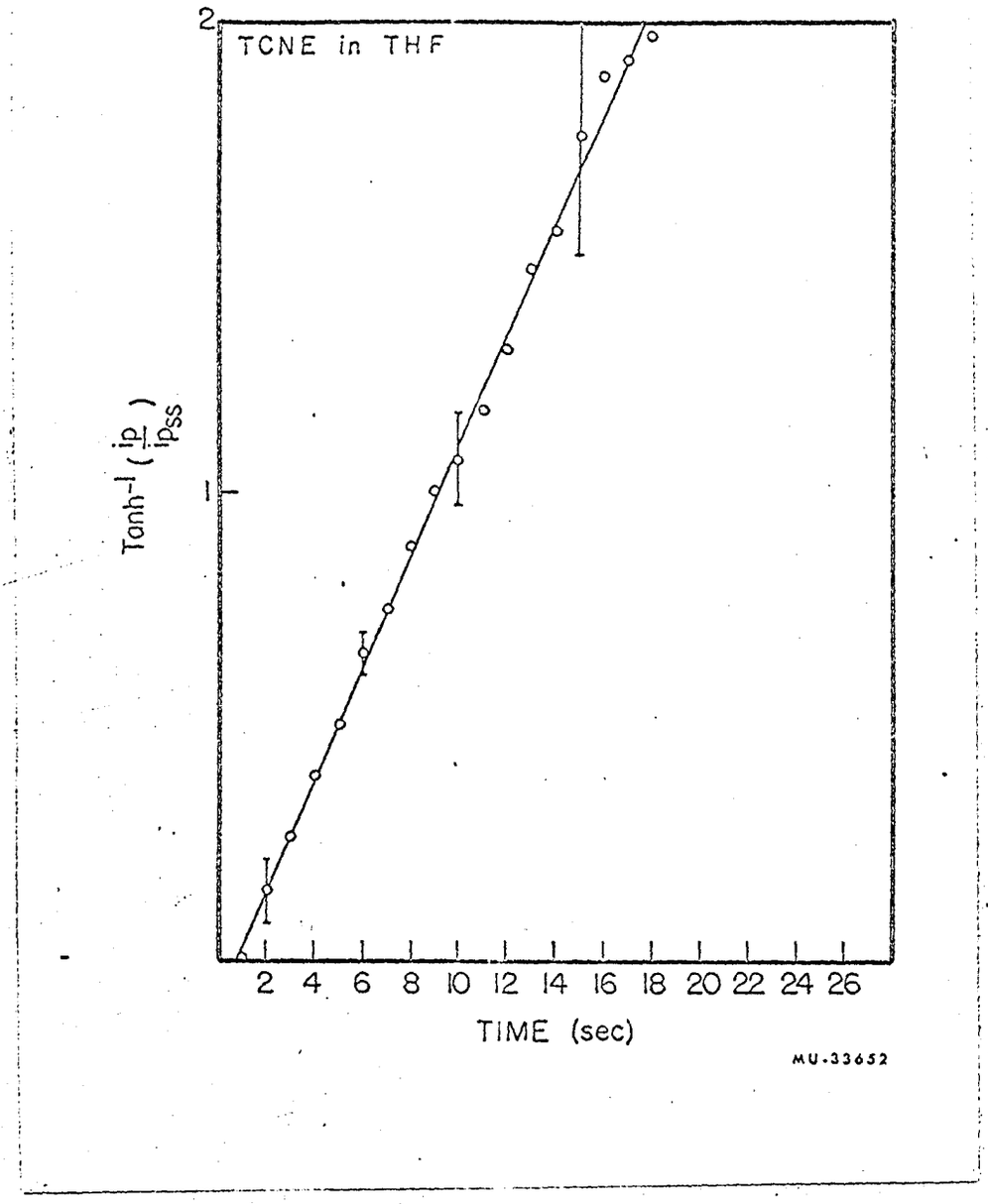
TCNE in THF
2
1
$\tanh^{-1}\left(\frac{i_p}{i_{pss}}\right)$
2 4 6 8 10 12 14 16 18 20 22 24 26
TIME (sec)
MU-33652

Fig. 12

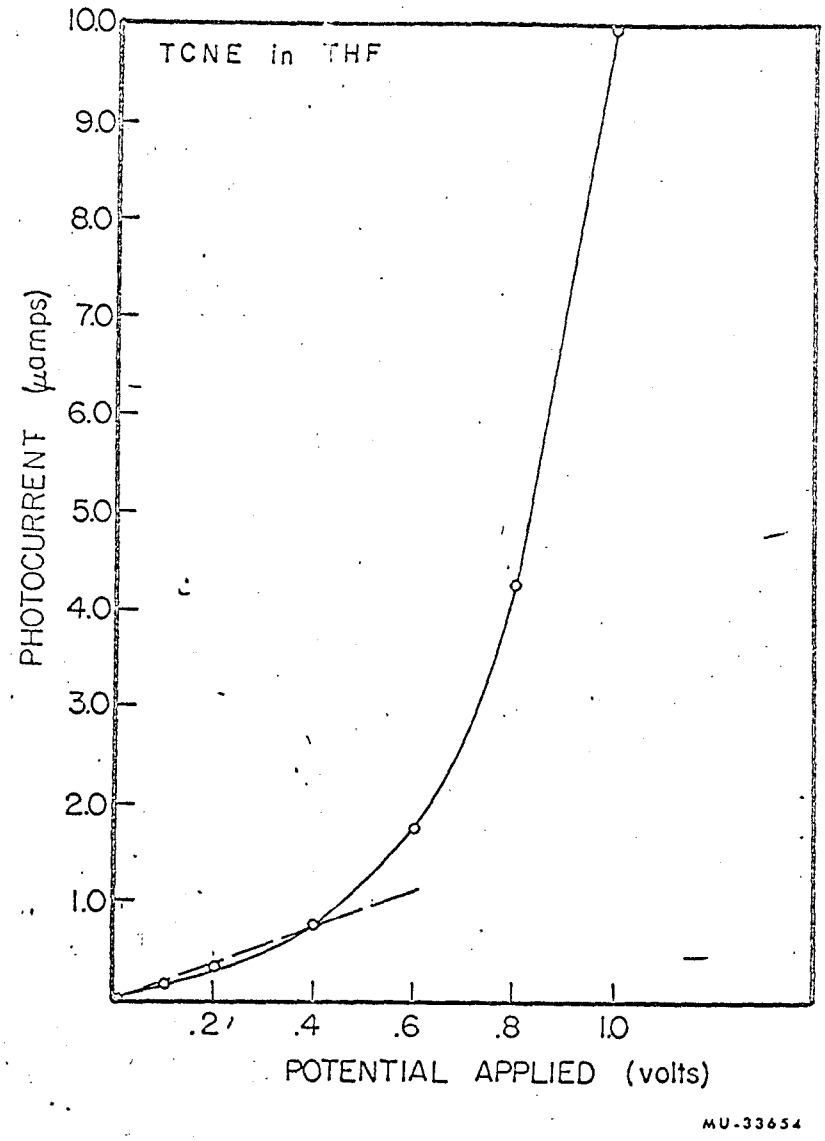
TCNE in THF
PHOTOCURRENT (μamps)
10.0
9.0
8.0
7.0
6.0
5.0
4.0
3.0
2.0
1.0
.2
.4
.6
.8
1.0
POTENTIAL APPLIED (volts)
MU-33654

Fig. 13